Multi-Resolution Analysis Features followed by Facial Part Detection for Face Recognition

Mustafa R. Ismael† and **Haider J. Abd**, Non-members

ABSTRACT

Face recognition is considered the main physiological and behavioral biometrics due to the following advantages; simplicity of the face capturing, feature uniqueness and distinctness, and availability of the image acquisition devices. In this paper, a new approach to face recognition system (FRS) utilizing the Two-Dimensional Discrete Multi-Wavelets Transform (2D DMWT) followed by Vector Quantization (VQ) to the detected face and facial parts (DF and DFP) is proposed. Faces and facial parts (Nose, Mouth, Left-Right Eyes) are detected in the preprocessing step. Face and facials are the main parts that represent each person in the feature extraction step. For dimensionality reduction and features selection, the 1-level of 2D DMWT decomposition is employed in the two representations. For each person in the second representation, four groups are constructed using the training poses, each group for each facial part. Furthermore, VQ and Kekre Fast Codebook Generation (KFCG) are applied to the detected faces and the four groups derived from the first and second representations, respectively. The Euclidean distance is utilized in the classification phase. Four databases, namely, YALE, FERET, FEI, and Georgia Tech. are used to test the FRS. These databases have different facial diversity, such as pose rotation, light condition, expressions, etc. K-fold Cross-Validation (CV) is utilized to analyze the experimental results. The proposed system improves the recognition rates and the storage requirement compared to the state-of-the-art approaches.

Keywords: Discrete Multiwavelet Transforms, Vector Quantization, Face Recognition, Facial Part Detection

1. INTRODUCTION

Biometrics, life measurements, is the unique physiological and behavioral characteristics of humans that can be employed to easily and quickly identify and authenticate individuals. In recent years, face recognition received considerable interest due to its applications in control, healthcare, security, and personal identification. In security systems, for example, face recognition is advantageous to identify the person who accesses fraudulent data, a particular building, breaching systems/ banking, etc. Face recognition is a fundamental matter in pattern recognition, signal and image processing (SP and IP), and computer vision. Previously, the individual was authenticated by a virtual/ physical domain that is based on tokens, keys, passwords, PINs, smart cards, etc. Since all of these virtual/ physical techniques are subjected to be stolen, misplaced, forgotten, etc., face recognition is unique, measurable, and permanent for every individual and it is promising to authenticate people's identity. Also, faces can be captured using a low-cost camera compared to other biometrics, such as retina, iris, etc. that are required costly and precise equipment [1], [2]. Although all the above benefits of face recognition, it is still a challenging task to accomplish due to several problems. The first one is the pose rotation in which the training poses have a rotation different from the testing poses. The second one is the dynamic face appearances that may cause different people associated of different ages. Variations in the illumination are another problem of face recognition in which these variations lead to change in the manifestation of the subjects. There are so many other problems, such as occlusion, unavailability of the whole face, low resolution, etc. All of the above problems lead to an increase in the dissimilarity between the training and testing poses. Hence, the recognition accuracies are reduced [3], [4].

Based on the above problems, many algorithms are used for face recognition. The Principal Component Analysis (PCA) is the widely used algorithm for face recognition. PCA is a signal representation technique that can extract facial basis (eigenfaces) from a covariance matrix derived from a set of training poses [5]. In 1991, Turk and Pentland [6] expanded the work presented by [7] and employed the eigenfaces algorithm to the face for face recognition. The performance of the system employing PCA suffers a noticeable degradation, especially for the databases that have different facial variations consisting of light conditions, rotation, expressions, etc. Hence, in 2014, Kundu et al [8] proposed fast ℓ_2 PCA to improve the performance of the PCA under facial variations.

Another subspace algorithm employed for face recognition is the linear discriminant analysis (LDA). LDA is a supervised method that uses the information obtained from the data class label. Contrary to PCA which projects the data along the direction of the maximum

Manuscript received on February 11, 2023; revised on March 9, 2023; accepted on August 22, 2023. This paper was recommended by Associate Editor Piya Kovintavewat.

The authors are with Department of Electrical Engineering, University of Babylon, Babel, Iraq.

†Corresponding author: eng.mustafa.rashid@uobabylon.edu.iq

Digital Object Identifier: 10.37936/ecti-eec.2024221.252947

variance, LDA pursues the directions for the maximum discrimination of the classes [9], [10]. Independent component analysis (ICA), the extended version of the PCA, is also a subspace method that is employed to the faces to identify individuals. ICA employs higher-order statistical data as compared to the PCA which only implements second-order statistics. Also, the basis images (functions) that are extracted by employing ICA are independent as compared to those basis images obtained from PCA which are considered uncorrelated [11].

Multi-resolution analysis (MRA), discrete wavelet transform (DWT), is widely and efficiently used in several fields. MRA is employed to accomplish noise reduction, dimensionality reduction, and feature selection. Based on the affirmative properties of the filters used in DWT, such as symmetry, orthogonality, etc., DWT can integrate with the 2 other algorithms/ transforms including ICA, PCA, DCT, etc. to accomplish prominent performance. The authors in [12] integrated both 2D PCA and 2D DWT for face recognition. In [12], Mukhedkar and Powalkar illustrated that the integrated methods (2D PCA/DWT) achieved better recognition rates compared to those rates resulting from employing 2D DWT or 2D PCA alone. In [13], ICA was employed to various levels of MRA decomposition and the recognition accuracies accomplished using the combined tools were higher than those rates obtained using the conventional algorithm DWT or ICA.

An extended version of DWT that is also based on MRA is the discrete multi-wavelets transform (DMWT). DMWT is broadly and successfully used for data compaction and signal representation. Akin to DWT, DMWT is employed for face recognition for dimensionality reduction, noise cancellation, and feature selection. Algorithms are combined to override the deficiency found in a single transform. Hence, the authors in [2] proposed different techniques that applied 2D DMWT integrated with FastICA followed by the ℓ_2 norm to facial parts for better facial representations. In [14], the authors applied the integrated tools, 2D PCA/DMWT, to infrared facial images. 2D PCA was employed to different levels of decompositions of DMWT and the results were weighted by the fisher discriminate method. A hybrid technique based on applying 3D DMWT to the integrated tools of 2D radon transform (2D RT)/2D DMWT was proposed in [15] for face recognition. The authors in [15] employed 2D DMWT to the different facial databases for feature selection and dimensionality reduction. Then, 2D RT was used to align the resulted 2D DMWT features around the origin and the 3D DWT was applied to localize the aligned features on one single band and achieve less storage. Vector Quantization (VQ) based on LBG (Linde, Buzo, and Gray) algorithm [16] and Discrete Cosine Transform (DCT) is widely and successfully used in data compression and data compaction. The authors in [17] employed the Eigen analysis algorithm (PCA) to low-frequency components that resulted from applying DCT to the facial images. Then, the Neural Network (NN) classifier was used for classification purposes.

Algorithms like LDA and PCA have some limitations when they are employed to face databases that have facial variations. To conquer these limitations, local facial features are promised to accomplish better performance [18]. To elicit the local facial features from the images, the extracting method can be accomplished either by partitioning a face into parts as in [2] or using proper tools. Aldhahab et al [19] extracted the local facial features (Nose, Mouth, Left-Right Eyes) by using facial part detection (FPD), which employs the Viola Jone algorithm. In [19], every person in the databases used was represented by four centroids, each for each facial part, regardless of the number of training poses; hence, they accomplished good results as well as less storage. Later, Aldhahab et al [20] extended their work by applying 2D DWT to each local facial feature for further dimensionality reduction and feature extraction. Then, four groups, each for each facial part, were constructed. Afterward, the VQ algorithm employing the algorithm presented by Kekre [21] in 2010 for codebook initialization was applied to each group to improve the performance of the system discussed in [19]. In [22], the facial images were divided into n overlapping parts to obtain the local features and PCA was employed in each part to achieve feature compaction. Although the complexity of the system proposed in [22] increased, the recognition rate accomplished was 92.4% based on the FERET database. Lu et al [23] employed one stage of Simulation Local Binary Feature Learning (SLBFL), an unsupervised learning method, to extract distinctive local features compared to those extracted features obtained using GWT and Local Binary Pattern (LBP). A new method based on applying 2D DMWT followed by VQ employing KFCG for codebook initialization to the detected faces and facial parts is proposed in this paper for face recognition. In this paper, each person in the databases used is described by two representations, face and facial parts (Nose, Mouth, Left-Right Eyes) representations. For each representation, 2D DMWT decomposition is implemented resulting in four frequency sub-bands, Low-Low (LL), Low-High (LH), High-Low (HL), and High-High (HH) pass filters. For both the detected face (first representation) and facial parts (second representation), all the discriminate information is contained in the LL sub-band. Therefore, the LL sub-band is considered for further partitioning into four sub-sub-bands while the other sub-bands are neglected. Then, the generated sub-sub-bands are averaged and the first dimensionality reduction and features selection are achieved. Then, only for the second representation, four groups for each person in the databases used, each for each part, are established using all training poses. Thereafter, the VQ exploiting KFCG and LBG algorithm is applied to the resulted representations for further reducing the storage and achieving better facial representation. Each person in the databases is represented by either

number of centroids based on the number of training poses (first representation) or four centroids resulting from four groups regardless of the number of training poses used (second representation). To do classification, Euclidean distance is employed. Four popularly and widely databases, namely, YALE [24], FERET [25], FEI [26], and Georgia Tech [27]. are used to examine the system proposed. These databases have facial variations, such as light conditions, pose rotations, makeup, facial details/ expressions, etc. The experimental results of the proposed system are evaluated using K-fold Cross-Validation (K-fold CV). The algorithm presented in this paper enhances the recognition rates and the storage requirements as compared with the state-of-the-art algorithms.

The rest of the paper is assembled as: Some mathematical backgrounds of the methods used are discussed in Section II. The system proposed is illustrated in Section III. In Section IV, the system's results and discussions are demonstrated. Finally, we conclude in Section V.

2. BACKGROUND: WAVELET, MULTIWAVELET, AND VQ

2.1 Discrete Wavelet and Multiwavelet Transform

The extended version of the Window Fourier Transform (WFT) is the Discrete Wavelet Transform (DWT). DWT is a crucial tool in several applications including feature selection, signal denoising, enhancements, compression, face recognition, etc. DWT is a powerful mathematical tool that is exploited in several areas of study, such as Image and Signal Processing (IP and SP), Computer Vision, Pattern Recognition, etc. [2], [28]. Filter banks utilizing both low and high pass filters arraying schematically are used to implement the DWT. Two sets of orthogonal functions called wavelet $\psi(t)$ and scaling function $\varphi(t)$ are the basis functions of the DWT, which satisfy the dilation equations:

$$\Phi(t) = \sum_{i=0}^{n-1} g_i \cdot \phi(2t-i), \tag{1}$$

$$\Psi(t) = \sum_{i=0}^{n-1} h_i \cdot \phi(2t-i), \tag{2}$$

where g_i and h_i are the discrete coefficients that define both DWT and wavelet filters $G(z) = \sum_{i=0}^{n-1} g_i \,.\, z^{-i}$ (low pass filter) and $H(z) = \sum_{i=0}^{n-1} h_i \,.\, z^{-i}$ (high pass filter) [28].

Four frequency sub-bands are resulted from applying 2D DWT, which is the extended version of the 1D DWT, to the 2D image. These sub-bands are related to the approximation coefficients (scaling functions) and the detail coefficients (wavelet functions) in which 2D DWT measures the intensity variations of an image along with different directions $\psi^V(x,y)$, $\psi^H(x,y)$ and $\psi^D(x,y)$, where $\psi(x,y)$ is the wavelet function of 2D DWT and V, H, and D are the Vertical, Horizontal, and Diagonal edges, respectively.

Similar to the traditional multi-resolution analysis (MRA), DWT, the MRA for multi-wavelet transform (2D DMWT) are utilizing P-scaling functions, $\phi_1(t-k)$, $\phi_2(t-k)$, …, $\phi_p(t-k)$, and P-wavelet functions, $\psi_1(t-k)$, $\psi_2(t-k)$, …, $\psi_p(t-k)$. Both multi-scaling and multi-wavelet functions, $\phi(t)$, and $\psi(t)$, can be expressed in a vector notation as:

$$\Phi(t) = \left[\phi_1(t),\, \phi_2(t), ..., \phi_P(t)\right]^T \in L^2(R)^P, \tag{3}$$

$$\Psi(t) = \left[\psi_1(t),\, \psi_2(t), ..., \psi_P(t)\right]^T \in L^2(R)^P. \tag{4}$$

Similar to the DWT case, the dilation and wavelet equations of the DMWT case are:

$$\Phi(t) = \sqrt{2} \sum_{k=-\infty}^{\infty} G_k \cdot \phi(2t-k), \tag{5}$$

$$\Psi(t) = \sqrt{2} \sum_{k=-\infty}^{\infty} H_k \cdot \phi(2t-k), \tag{6}$$

where both G_k and H_k are P×P matrices for every integer k. Based on the filter banks, G_k and H_k are related to the low pass and high pass filters, respectively [29], [30]. In this paper, we used P = 2 which is related to one of the famous multi-wavelets filter banks called GHM based on Geronimo, Hardin, and Massopust (GHM) [31].

The filter bank, GHM, is based on two scaling functions $\boldsymbol{\Phi}(t) = \left[\phi_1(t)\ \ \phi_2(t)\right]^T$ and wavelet functions $\boldsymbol{\Psi}(t) = \left[\psi_1(t)\ \ \psi_2(t)\right]^T$. Multi-wavelets filter, GHM, not only carries all the advantages of the traditional wavelet, but also it has the properties of symmetry, orthogonality, and linear phase simultaneously [29].

For the GHM case, both dilation equation Eq. (5) and wavelet equation Eq. (6) are expressed as [29]:

$$\Phi = \begin{bmatrix}\phi_1(t)\\ \phi_2(t)\end{bmatrix} = \sqrt{2}\sum\nolimits_k G_k \cdot \begin{bmatrix}\phi_1(2t-k)\\ \phi_2(2t-k)\end{bmatrix}, \tag{7}$$

$$\Psi = \begin{bmatrix}\psi_1(t)\\ \psi_2(t)\end{bmatrix} = \sqrt{2}\sum\nolimits_k H_k \cdot \begin{bmatrix}\phi_1(2t-k)\\ \phi_2(2t-k)\end{bmatrix}. \tag{8}$$

Readers refer to [29]–[31] for further details about the GHM filter. Four affirmative properties for the filter bank, GHM, are mentioned in [29], [30]. H_k & G_k of the GHM filter and for k = 0, 1, 2, 3 are written as [29], [30]:

$$H_0 = \begin{bmatrix} \frac{3}{5\sqrt{2}} & \frac{4}{5} \\ \frac{-1}{20} & \frac{-3}{10\sqrt{2}} \end{bmatrix} \qquad H_1 = \begin{bmatrix} \frac{3}{5\sqrt{2}} & 0 \\ \frac{9}{20} & \frac{1}{\sqrt{2}} \end{bmatrix}$$

$$H_2 = \begin{bmatrix} 0 & 0 \\ \frac{9}{20} & \frac{-3}{10\sqrt{2}} \end{bmatrix} \qquad H_3 = \begin{bmatrix} 0 & 0 \\ \frac{-1}{20} & 0 \end{bmatrix}$$

$$G_0 = \begin{bmatrix} \frac{-1}{20} & \frac{-3}{10\sqrt{2}} \\ \frac{1}{10\sqrt{2}} & \frac{3}{10} \end{bmatrix} \qquad G_1 = \begin{bmatrix} \frac{9}{20} & \frac{-1}{\sqrt{2}} \\ \frac{-9}{10\sqrt{2}} & 0 \end{bmatrix}$$

$$G_2 = \begin{bmatrix} \frac{9}{20} & \frac{-3}{10\sqrt{2}} \\ \frac{9}{10\sqrt{2}} & \frac{-3}{10} \end{bmatrix} \qquad G_3 = \begin{bmatrix} \frac{-1}{20} & 0 \\ \frac{-1}{10\sqrt{2}} & 0 \end{bmatrix}$$

Applying DMWT to an image is requiring to construct of the transformation matrix (T), which can be written as [30], [32]:

$$T = \begin{bmatrix} H_0 & H_1 & H_2 & H_3 & 0 & 0 & \cdots \\ G_0 & G_1 & G_2 & G_3 & 0 & 0 & \cdots \\ 0 & 0 & H_0 & H_1 & H_2 & H_3 & \cdots \\ 0 & 0 & G_0 & G_1 & G_2 & G_3 & \cdots \\ \vdots & \vdots & \vdots & \vdots & \vdots & \vdots & \cdots \end{bmatrix}$$

Akin to DWT which partition the image into four frequency sub-bands, DMWT is further dividing each main sub-band resulted by DWT into four sub-sub-bands. The relation between levels of decompositions of DMWT and the number of the sub-bands is mathematically expressed as $4 + 12 \times D$, where D is the required level of DMWT decompositions. In contradiction to DWT that is required a scalar input, DMWT requires the vector input in the convolution steps. This is due to both H_k and G_k for the filter bank, GHM, are $P \times P$ matrix., Thus the input image (signal) has to pass through prefiltering steps (preprocessing). To make an image (signal) compatible with the transformation matrix used (GHM case), the vector-valued signal is obtained from the scalar signal in the prefiltering step to accomplish better results [2], [29], [30], [33].

In this paper, the input image is resized into $R \times R$, where R is the power of two dimensions to be consistent with the transform used. There are various methods for prefiltering (preprocessing) explained in [33], [34]. Two very well-known preprocessing are called over-sampled scheme preprocessing (repeated row preprocessing), which produced R-length 2-vector, and critically-sampled scheme preprocessing (approximation-based preprocessing), which produced R/2 length 2-vector. In this paper, the critically sampled scheme preprocessing that produced R/2 length 2-vector is employed [29], [30], [33]. The algorithm of applying 2D DMWT to an image employing an approximation-based approach (critically sampled scheme preprocessing) is explained in detail in [35].

2.2 Vector Quantization (VQ)

OS-ELM is an incremental learning algorithm, which was proposed by N.Y. Liang [16]. It is an incremental learning version of the Extreme Learning Machine [24]. It is applied to a single hidden layer feed-forward neural network as shown in A very well-known algorithm that is used in the field of image processing, especially in image compression is vector quantization. The first well-known approach implemented the VQ is invented by Y. Linde, et al. in 1980 and it is called the LBG algorithm based on the scientists Y. Linde, A. Buzo, and R. Gray [16]. LBG algorithm is based on LIoyd approach. In such an algorithm, LBG, the image is partitioned into blocks and each one is replaced by a centroid or codeword, and the sets of the centroids are called a codebook. The LBG algorithm was introduced to accomplish high compression rates in addition to reducing the error to the lowest rates. In the LBG algorithm, the replacing process between the centroid and the image partition (block) is based on the resemblance between them. Several parameters should be considered when designing the VQ. The dimensions of the centroids (codewords) have to be the same as the image blocks. The size of the codebook, and the number of codewords, are chosen to minimize the error between the input image and the quantized one. Increasing the number of the codewords results in decreasing the distortion error factor between the input image and the quantized version, but at the same time, it is required more space. The distortion criterion, which is Modified Itakura-Satio, norm-based distance criteria, Mean Squared Error (MSE), and codebook initialization are the last two parameters required in designing the VQ. All the above parameters have to be optimized at the same time [36].

To implement the VQ, it is required to select the dimensions of the codeword (centroid), and assume $g \times h$ is the size of the codeword. Then, the input image has to be partitioned into non-overlapping blocks with the same dimensions of the codeword ($g \times h$). The first centroid is calculated by averaging all the image blocks. Based on the LBG approach, the second process of finding the next centroid is by adding and subtracting a small number called ε to/from the first centroid. To update these two centroids using the LBG algorithm, each updated new centroid is calculated by averaging all image blocks that were closed to that centroid from the other. Again, to find the four centroids from the updated ones, the ε is added and subtracted to/from the two new centroids. Again, the updated four centroids are found by averaging all image blocks that are closer to each centroid. The process of splitting is stopped when the required number of centroids (C) is achieved.

In this paper, the MSE is used to measure the distances, i.e., the total distortion. The initialization process of the LBG algorithm is time-consuming. Thus, the algorithm presented by Kekre et al. [21] in 2010 is an alternative to the LBG algorithm, where the initial codebook is computed faster than using the LBG algorithm. The Kekre Fast Codebook Generation KFCG, which is presented by [21] and is used in this paper, also begins with finding the first codeword (centroid) by computing the mean of all the image blocks. Then the splitting process is beginning by comparing the first element in the mean block and the counterpart in the image blocks. Hence, the image blocks are divided into two sets based on whether or not the first element in the image block is greater/less than the first value in the mean block. Then, the two groups of the image blocks are partitioned into four groups based on the computed two means. This is done by implementing the same comparison process above, but now with different values.

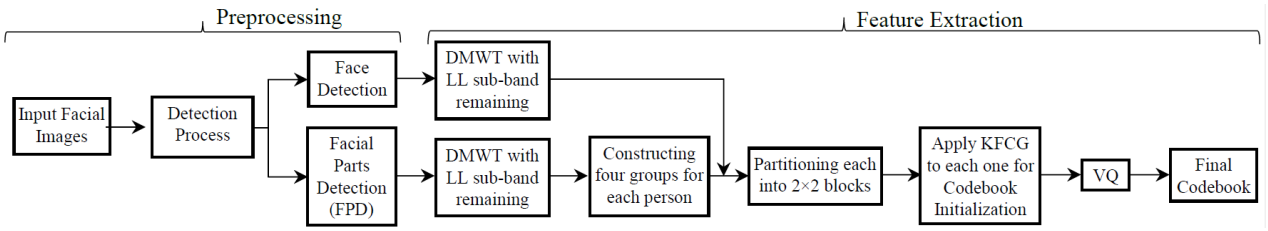

(a) Training Mode with the Preprocessing and Feature Extraction Steps.

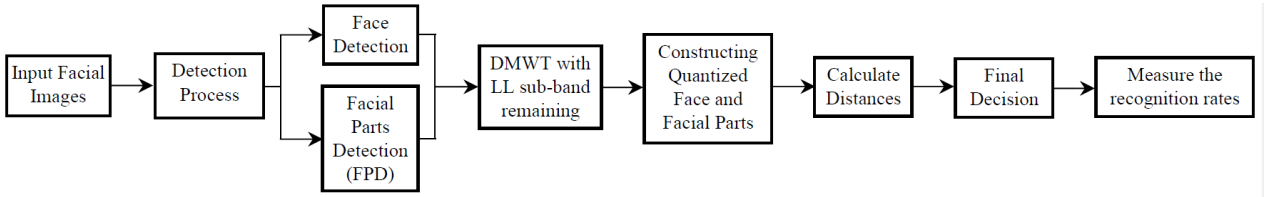

(b) Classification Mode.

***Fig. 1**: The Proposed System.*

(a) YALE

(b) FERET

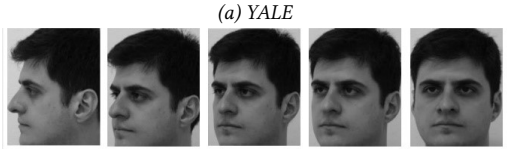

(c) FEI

(d) Georgia Tech.

***Fig. 2**: Samples of databases used.*

The process, computing the mean of each partitioned group, comparison, and splitting, is stopped when the required number of centroids is accomplished. The final codewords (centroids) are considered to be the initial codebook.

3. PROPOSED SYSTEM (PS)

In this section, the proposed system (PS) is demonstrated. There are three main phases in the PS: Preprocessing, Feature Selection, and Classification as shown in Fig. 1. In the first phase, faces and facial parts (FP), which are Nose, Mouth, and Left-Right Eyes, are detected using the Viola-Jones algorithm. Then, the detected faces and FP are resized into appropriate dimensions. Reduction in dimensionality and feature selection is accomplished in the second phase. In the third phase, the discriminant selected features obtained in the second phase are utilized to recognize the person in a set of various databases using the Euclidean distance. In this paper, four databases are exploited to investigate the performance of the proposed system. These databases contain different facial variations, such as face rotations, face details, different illuminations, different facial expressions, etc. as shown in Fig. 2. To analyze the experimental results, K-fold Cross-Validation (CV) is employed.

The PS starts with selecting the parameters of the VQ as follows:

1) The size of the centroids g and h are 2×2 ($g \times h$).
2) The length of the codewords (codebook) is 8 (L).
3) The distortion error is measured by the Mean Square Error (MSE).
4) The initialization of the codebook is accomplished using KFCG.

3.1 Preprocessing

- The first step of the preprocessing is detecting faces in the images by employing Viola-Jones Algorithm. MATLAB 2019 using the computer vision toolbox, vision. ***CascadeObjectDetector*** is employed to process this step. Fig. 3 is illustrating an example of detecting faces. The dimensions of all detected faces are 128×128 for YALE and Georgia Tech. databases, 64×64 for the FEI database, and 32×32 for the FERET database.
- The second step aims to find the facial parts, represented by Nose, Mouth, and Left-Right Eyes. This is accomplished by employing FPD to the detected faces resulting in step 1. A sample of the detected parts is shown in Fig. 3. The dimensions of all detected facial parts are 32×32 for YALE, Georgia Tech., and FERET databases and 64×64 for the FEI database.

(a) (b) (c) (d)

***Fig. 3**: Facial parts detection using Viola-Jones algorithm.*

(a) Person No.1 (b) Person No.2 (c) Person No.3 (d) Person No.4

***Fig. 4**: Applying 2D DMWT to Detected Faces of YALE Database.*

3.2 Feature Extraction

The feature extraction stage is considered an intrinsic step in every recognition system and data mining. Designing an efficient face recognition system under different facial variations, such as facial expressions, various face rotations, illuminations, makes up, facial details, etc. is considered a challenging problem.

Dimensions of faces in the images play an important role in the recognition accuracy and computational complexity since faces with large dimensions contain a lot of redundant information. Therefore, dimensions can have a direct effect on overall system performance.

Hence, the target of this stage is to obtain relevant and substantial features from the original face images that can lead to better representation of the face images, less computational complexity, fewer dimensions, and hence high recognition rates compared to the results of the original features. Therefore, the proposed system is employed to accomplish the following:

1) The Multi-resolution Analysis based on Multi-Wavelets Transform is employed for:
   a) Reducing the dimensionality of the databases used, hence achieving fewer storage requirements (data compression).
   b) Image denoising and enhancement.
   c) Localizing most of the energy of the input signal (image) in one single sub-band (low-frequency sub-band).
2) Vector Quantization is utilized for:
   a) Representing the input Signal (facial images) by only centroids.
   b) Compressing data (dimensionality reduction) [32].

There are two modes in the proposed system: a) Training mode. b) Testing mode.

The feature extraction steps are applied to the two modes. After applying the preprocessing steps to the input face image, the resultant processed images (the face and facial parts) have the power of two dimensions, which are chosen to be consistent with the transform used (2D DMWT). The first step in the feature extraction phase is employing a 1-level of 2D DMWT decompositions to the processed images (face and facial parts) as demonstrated in Fig. 4. All faces and facial parts in all images that are belonging to all databases used (FERET, YALE, Georgia Tech., and FEI) are partitioned into four frequency sub-bands, labeled as LL, LH, HL, and HH sub-bands. Where L and H are related to low pass and high pass filters, respectively. For the detected faces of the subjects in YALE, FERET, and Georgia Tech. databases, each sub-bands have 64×64 dimensions. For the detected faces of the subjects in the FEI database, each sub-bands have dimensions of 128×128. Concerning the facial parts of the subjects in YALE, Georgia Tech., and FERET databases, the dimensions of all sub-bands are 16×16. Moreover, the dimensions of the sub-bands for the facial parts of the subjects in the FEI database are 32×32.

Also, as shown in Fig. 4 that each sub-band (LL, LH, HL, and HH) is further divided into four sub-sub-bands. For the case of the detected faces of the subjects in YALE, Georgia Tech., and FERET databases, each sub-sub-band has 32×32 dimensions while the dimensions of each sub-sub-band in the FEI database are 64×64. Also, each sub-sub-band of the detected facial parts in YALE, Georgia Tech., and FERET databases has dimensions of 8×8 while the dimensions of each sub-sub-band in the FEI database are 16×16. As seen in sub-Figs. 4(a) - 4(d) that most of the detected face and facial parts energy is localized in one single sub-band, which is related to the LL frequency sub-band. Therefore, the approximation coefficients (LL sub-band) will be preserved and all other detail coefficients (LH, HL, and HH sub-bands) that have Vertical, Horizontal, and Diagonal directions of the originally detected faces and facial parts are excluded.

Then, the next step is finding the mean of the maintained sub-sub-bands. This is done by averaging all the sub-sub-bands in the remaining LL frequency sub-band as expressed in Eq. (9) as:

$$Mean_{features} = \frac{L_1L_1 + L_1L_2 + L_2L_1 + L_2L_2}{4} \quad (9)$$

The mean features of the detected face obtained by Eq. (9) have dimensions of 32×32 for YALE, Georgia Tech., and FERET databases and 64×64 for the FEI database. Also, the dimensions of the mean features resulting from the detected facial parts are 8×8 for YALE, Georgia Tech., and FERET databases and 16×16 for FEI databases. The next step is forwarding the mean features of both detected faces and facial parts to the Vector Quantization (VQ) to accomplish further features' reduction/compaction and better face/ facial parts representations.

For each input face image belonging to each person in the databases used, there are two representations. The first one corresponds to the detected face and the other one is related to the detected facial parts.

To apply the VQ to the first representation, the extracted features obtained from the detected faces are

(a) Nose *(b) Mouth* *(c) R_Eye* *(d) L_Eye*

***Fig. 5**: Six training poses of person No. 4 in the YALE database.*

divided into non-overlapping partitions (blocks). Each partition is with dimensions of 4×4 (q×s). The initial step in the VQ is finding the mean, which has the same partitions' dimensions (4×4) which can be expressed as follows:

$$K = \frac{dimensions\ of\ the\ extracted\ features}{q \times \mathrm{s}} \tag{10}$$

$$T_r = \frac{T_r^{k_1} + T_r^{k_2} + \cdots + T_r^{K}}{K} \tag{11}$$

where K refers to the number of partitions. Hence, $K = \frac{32\times32}{4\times4} = 64$ partitions for YALE, Georgia Tech., and FERET databases while $K = \frac{64\times64}{4\times4} = 256$ partitions for FEI databases. T_r is the r^{th} elements in the k^{th} partition, $k \in Z : k \in \{1, 2, \cdots, K\}$. Among all partitions, Tr is the r^{th} average of all elements, such that $r \in Z : r \in \{1, 2, \cdots, q \times s\}$. After finding the first mean obtained by Eq. 10 and Eq. 11, the initial codebook is generated using the method explained in [21] in 2010. Afterward, the first split of the non-overlapping partitions into groups is based on comparing the values of the elements in the partitions with the corresponding ones in the mean. As a result, the initial codebook is computed after log2 L = 5 splits. Where L is 32, which is the codebook size. Readers refer to [21] for further details about the splitting process. Then, the new codebook is generated using the LBG algorithm. In each split, the codeword (centroid) update process is accomplished by summing all the data partitions that were encoded using that codeword (centroid) and dividing by their total number. The procedures of computing the codebook are repeated as many as the number of training poses each time the number of individuals in all databases is used.

To apply the VQ to the second representation, the extracted mean features of the detected facial parts are arranged into four groups (sets) for each person in the database, each group belongs to one facial part using various training poses. An example of organizing four groups using six different samples of poses of person No. 4 of the YALE database is illustrated in Fig. 5.

The sets (groups) of extracted mean features of each facial part are shown in Fig. 5. Let P is the number of the training poses and $X = \sqrt{P}$. If the size of P is a^2, where $a \in Z > 0$. Then, X is an integer number ($X \in Z > 0$), called a perfect square, and the set (group) is organized as a square. Otherwise, the set is arranged in a rectangular form ($X \in Q > 0$). In general, the dimensions of the set are $N \times M$. When X is an integer value, N and M are equal.

Then, the four sets (groups) are forwarded to the VQ for further data compression and better facial part representation. The steps of the VQ are applied to each set (group) individually. As mentioned in the first representation for implementing the VQ, every set is divided into non-overlapping partitions. Each non-overlapping partition has dimensions equal to the codeword dimensions, which are 2×2 ($q \times s$). Hence, as mentioned, the first step is finding the mean across all non-overlapping partitions using Eq. 10 and 11. The dimensions of the resulted mean are the same dimensions of the codeword (2×2). After finding the mean of all non-overlapping partitions and employing the algorithm discussed by Kekre [21], KFCG, the initial codebook is constructed. In each set (group), the blocks are split into two sub-sets based on comparing the values in each block with their corresponding ones in the mean. Since the length of the codebook L = 8, the initial codebook is constructed after $log_2 L = 3$ splits. Subsequently, the LBG algorithm determines the updated new codebook.

In each split, the updated codeword is computed by summing all blocks in each sub-set that were encoded using that codeword and dividing by their total number. The execution steps of computing the codebook are reiterated by 4-times for each individual since there are 4 sets to represent each individual in the training mode. Hence, the steps of finding the codebook are repeated by *4 × No. of individuals in the databases × No. of databases used.* In this representation, there are 4 codebooks, each for each set shown in Fig. 5, to represent each person in the database regardless of the number of poses used in the training mode. Each codebook contains 8 centroids (codewords), each with dimensions of 2×2. Hence, the final features extracted for each person using this representation have dimensions of $4 \times 2 \times 2 \times 8 = 128$.

The dimensionality reduction is measured as:

$$Reduction\% = \left(1 - \frac{4 \times Codebooks\ Dimensions}{P \times poses'\ Dimensions}\right) \times 100 \tag{12}$$

For the example shown in Fig. 5, individual No. 4 in the YALE database is efficiently represented by 4 codebooks $4 \times 2 \times 2 \times 8$. The dimensionality reduction is:

$$Reduction\% = \left(1 - \frac{4 \times 2 \times 2 \times 8}{6 \times 243 \times 320}\right) \times 100\% = 99.97\%$$

Hence, using this method of representing the individual in the database leads to achieving better facial representation and data compaction in which fewer storage requirements are accomplished.

3.3 Recognition

As shown in Fig. 1(b), the input (test image) is passed through the same steps, which are preprocessing and feature extractions that are demonstrated in Fig. 1(a) (training mode). Each input (tested image) is passed through the detecting process. The result is the detection

of the face and facial parts, each is evaluated separately. Hence, all the codebooks of the subjects that are resulted from the first representation are used to reestablish the quantized version of the test detected face. Also, all the codebooks of all individuals that are obtained from the second representation are used to reconstruct the quantized version of each of the test detected facial parts (Nose, Mouth, and Left-Right Eyes). For recognition purposes, the distances between the tested detected face/ facial parts and the quantized one are computed. Hence, there are two types of distances. One related to the test detected face and the quantized one. The other one is between each test-detected facial part and the quantized one. Then, locate the person that is linked to the minimum distance. Since there are two types of distances, there are five results, each belonging to the test detected face/ facial parts (mouth, nose, left and right eyes). The decision is made based on the following:

1) Find the minimum distance among all the results. Then the person whose codebook has the minimum distance is stated as the matched one.
2) Investigate whether the matched one is the correct one or not.

For the second representation:

1) Test each facial part separately.
2) Find the minimum distance among all the results.
3) Repeat steps 1 and 2 for other facial parts.
4) There are four results related to four facial parts.
5) To identify the exact person, the voting criteria are employed.
6) The tested pose (tested input image) is correctly matched the exact person if only if three of the facial parts are rightly identified.

To measure the accuracies of the recognition system, the following equation is used:

$$Accuracy\% = \frac{T.P.C.M}{T.P.T.M} \times 100 \tag{13}$$

where $T.P.C.M$ refers to the total number of the tested poses correctly matched. $T.P.T.M$ states the number of poses used in the testing mode.

4. EXPERIMENTAL RESULTS AND DISCUSSION

In this section, the experimental results of the system proposed are discussed and presented. The system proposed is also compared with the existing approaches. YALE, Georgia Tech., FERET, and FEI are the databases employed to evaluate the system proposed. These databases have a lot of facial variations, such as illuminations, rotations, makes up, facial expressions, facial details, etc. in this proposed system, K-fold Cross-Validation (K-fold CV) is used to analyze the results. Also, it can be stated that when the training poses were used in the testing mode, the system proposed achieved 100% accuracy in all databases used.

***Table 1**: Experimental Results obtained using the YALE Database.*

K-Fold	Recognition rates for the First Representation (Face)			
	Proposed System	VQ FPD [19]	DWT/PCA-L [37]	GLCM/NN [38]
K=2	94.7%	94.2%	92%	87%
K=3	95.9%	95.4%	93.6%	91.3%
K=5	97.1%	96.6%	94.7%	94%
K-Fold	Recognition rates for the Second Representation (Facial Parts)			
	Proposed System	VQ FPD [19]	DWT/PCA-L [37]	GLCM/NN [38]
K=2	95.8%	95.75%	92.6%	88%
K=3	97.7%	97.6%	94%	92.1%
K=5	98.8%	98.51%	95.8%	96%

***Table 2**: Experimental Results obtained using the GT Database.*

K-Fold	Recognition rates for the First Representation (Face)			
	Proposed System	VQ FPD [19]	DWT/PCA-L [37]	GLCM/NN [38]
K=2	94.4%	94%	85%	87.9%
K=3	96.5%	95.8%	91.8%	92%
K=5	97.6%	96.6%	94.8%	94.3%
K-Fold	Recognition rates for the Second Representation (Facial Parts)			
	Proposed System	VQ FPD [19]	DWT/PCA-L [37]	GLCM/NN [38]
K=2	95.6%	95.3%	90.4%	90.1%
K=3	97.5%	97%	92.6%	92.6%
K=5	98.7%	98%	95.1%	94.8%

4.1 The YALE Database

There are 11 different poses linked to each person in the YALE database. The resolution of each pose is 320 × 243 pixels in GIF format. There are 15 persons, each has different facial diversities.

These diversities are facial details, illumination, and expressions (happy, sad, surprised, sleepy, and wink) [39]. The results of the two representations compared with the other approaches are shown in Table 1. The system proposed achieved better results as compared with some of the existing approaches.

4.2 The Georgia Tech. Database

In Georgia Tech. database, there are 50 persons, each with 15 different poses. Each pose has a resolution of 640 × 480 pixels in JPEG format. In this database, each pose has different facial variations, such as light conditions, scale, and facial expressions. All images show tilted and/ or frontal faces. The experimental results of the GT. database compared with the other methods are shown in Table 2.

***Table 3**: Experimental Results obtained using the FERET Database.*

K-Fold	Recognition rates for the First Representation (Face)			
	Proposed System	VQ FPD [19]	DWT/PCA-L [37]	GLCM/NN [38]
K=2	94.5%	94%	90.5%	88.3%
K=3	96.1%	95.7%	92.7%	91.1%
K=5	97.4%	97%	94.6%	93.7%
K-Fold	Recognition rates for the Second Representation (Facial Parts)			
	Proposed System	VQ FPD [19]	DWT/PCA-L [37]	GLCM/NN [38]
K=2	95.3%	95.1%	91.4%	90.2%
K=3	96.8%	96.83%	94.1%	93.2%
K=5	98.2%	97.98%	95.3%	94.8%

***Table 4**: Experimental Results obtained using the FEI Database.*

K-Fold	Recognition rates for the First Representation (Face)			
	Proposed System	VQ FPD [19]	DWT/PCA-L [37]	GLCM/NN [38]
K=2	94.3%	93.8%	89.9%	87.9%
K=3	96.4%	95.6%	92.3%	92%
K=5	97.5%	96.4%	94.8%	94.3%
K-Fold	Recognition rates for the Second Representation (Facial Parts)			
	Proposed System	VQ FPD [19]	DWT/PCA-L [37]	GLCM/NN [38]
K=2	95.4%	95.18%	90.7%	90.1%
K=3	97.2%	96.54%	93.8%	92.6%
K=5	98.6%	97.92%	95.1%	94.8%

4.3 The FERET Database

There are 200 subjects in the FERET database, each with 11 different poses. Each pose in the FERET database has a resolution of 256 × 384 pixels in TIFF format. The poses in the FERET have different light conditions, rotations, facial expressions, and glasses /no glasses [40], [41]. Table 3 shows the results of the proposed system compared with some of the existing approaches. The results achieved has similar performance as in the previous databases when compared with the existing methods.

4.4 The FEI Database

The FEI database comprises 200 subjects, each subject consists of 14 different poses. Each pose has 640 × 480 pixels resolution in JPG format. These poses contain different facial expressions, -90 deg to +90 deg face rotation [42]. In this paper, we used the grayscale version of this database. The experimental results of the proposed system are presented in Table 4. Also, the system is compared with the other state-of-the-art approaches. The system proposed based on the face and facial part representations accomplished better results compared with the other methods.

The objective of applying face and facial part detection in the preprocessing step is to eliminate the redundant information that is in common among all poses in the databases used, such as hair, etc. In addition, a detection step is employed to highlight the local facial parts (Nose, Mouth, Left-Right Eyes) and reduce the storage requirements. The desirable and favorable properties of DMWT, represented by orthogonality, symmetry, and a high order of approximation, cannot accomplish at the same time using traditional wavelets. Also, the dimensionality reduction obtained using DMWT is higher compared with those obtained by using DWT. The number of subbands resulting from levels of decompositions is $3\times L + 1$ and $4 + 12 \times L$ for DWT and DMWT, respectively. Hence, the system proposed achieved fewer storage requirements in comparison to the storage accomplished by [12], [13], [43]. Every person in the databases used is represented by the features extracted from the training poses. In [44], [45], every person was represented by the extracted features (centroids) from each training pose times the number of poses used in the training phase. In [44], [45], the irrelevant information (unnecessary facial information) was included since the whole face image was employed in the system proposed. However, in this paper, the detection process and the grouping technique are utilized to highlight the local and desirable facial parts (Nose, Mouth, Left-Right Eyes), in which all the unnecessary information is illuminated. furthermore, this leads to accomplishing fewer storage requirements compared to those obtained in [44], [45]. Each person in the database is represented by $4 \times centroid$ regardless the number of training poses. Therefore, detecting process and grouping technique are not only achieved better facial representation but also accomplished higher dimensionality reduction compared to those obtained by [44], [45].

For further dimensionality reduction and better facial representation, the VQ is employed in this paper. Also, using the KFCG algorithm for codebook initialization produces centroids that are better at representing the face and facial parts compared to those centroids resulting from the LBG algorithm. This leads to accomplishing better performance and results using KFCG than the performance and results achieved by the LBG. The results of the method proposed, Tables 1-4, outperformed the results presented using other approaches.

5. CONCLUSION

In this paper, face and facial parts detection in conjunction with the two-dimensional Multi-resolution Analysis (2D DMWT) and Vector Quantization were proposed for face recognition. Face, Nose, Mouth, and Left-Right Eyes were detected using FD and FPD processes. Hence, two representations were constructed, one is related to the face and the other one is corresponding to the facial parts. 2D DMWT was employed for each

representation and only the LL (low frequency) sub-band was retained. For the second representation and each person, the training poses were used to construct the four groups, each for each facial part. For further dimensionality reduction and facial discrimination, the VQ employed KFCG for codebook initialization was employed to the LL sub-band resulting from the first representation and the four groups resulted from the second representation. For the first representation, the final features extracted for each pose of each person in the databases used were of $4 \times 4 \times 32$ dimensions. furthermore, for the second representation, the final features extracted for each person in the databases used were 4 centroids ($4 \times 2 \times 2 \times 8 = 128$) dimensions. Each centroid in the second representation is linked to each group, which is corresponding to each facial part. Each representation was tested separately. Four databases that have different facial variations, such as different illuminations, rotations, make-up, occlusions, facial expressions, etc. were used to examine the system proposed. K-fold CV was employed to analyze the results of the two representations. In this contribution, the system proposed two representations and accomplished better face and facial parts representations, higher dimensionality reduction, as a result, higher recognition rates in comparison to those achieved by other methods, see Tables 1-4.

Conflict of interest: The author declares that they have no known competing financial interests or personal relationships that could have appeared to influence the work reported in this paper.

Data availability: The datasets analyzed during the current study are available in the following repositories:
[YALE] repository
[http://vision.ucsd.edu/content/yale-face-database],
[FERET] repository
[https://www.nist.gov/programs-projects/face-recognition-technology-feret],
[FEI] repository
[https://fei.edu.br/∼cet/facedatabase.html],
[Georgia Tech] repository
[http://www.anefian.com/research/face_reco.htm].

REFERENCES

[1] R. Jafri and H. R. Arabnia, "A survey of face recognition techniques," *J. Inf. Process. Syst.*, vol. 5, no. 2, pp. 41–68.

[2] A. Aldhahab and W. B. Mikhael, "Face Recognition Employing DMWT Followed by FastICA," *Circuits, Syst. Signal Process.*, vol. 37, no. 5, pp. 2045–2073, May 2018.

[3] Y. Xu et al., "Data uncertainty in face recognition," *IEEE Trans. Cybern.*, vol. 44, no. 10, pp. 1950–1961.

[4] M. M. Karimi and H. Soltanian-Zadeh, "Face Recognition: A Sparse Representation-based Classification using Independent Component Analysis," in *IEEE Sixth International Symposium on Telecommunications (IST)*, pp. 1170–1174.

[5] K. Papachristou, A. Tefas, and I. Pitas, "Symmetric Subspace Learning for Image Analysis," *IEEE Trans. Image Process.*, vol. 23, no. 12, pp. 5683–5697, Dec. 2014.

[6] M. A. Turk and A. P. Pentland, "Face recognition using eigenfaces," in *IEEE Proceedings Computer Society Conference on Computer Vision and Pattern Recognition (CVPR)*, Jun. 1991, pp. 586–591.

[7] L. Sirovich and M. Kirby, "Low-dimensional procedure for the characterization of human faces," *J. Opt. Soc. Am. A*, vol. 4, no. 3, pp. 519–524, Mar. 1987.

[8] S. Kundu, P. P. Markopoulos, and D. A. Pados, "Fast computation of the L1-principal component of real-valued data," in *2014 IEEE International Conference on Acoustics, Speech and Signal Processing (ICASSP)*, May 2014, pp. 8028–8032.

[9] A. Iosifidis, A. Tefas, and I. Pitas, "On the Optimal Class Representation in Linear Discriminant Analysis," *IEEE Trans. Neural Networks Learn. Syst.*, vol. 24, no. 9, pp. 1491–1497, Sep. 2013.

[10] H. M. Moon, D. Choi, P. Kim, and S. B. Pan, "LDA-based face recognition using multiple distance training face images with low user cooperation," in *2015 IEEE International Conference on Consumer Electronics (ICCE)*, Jan. 2015, pp. 7–8.

[11] M. S. Bartlett, J. R. Movellan and T. J. Sejnowski, "Face recognition by independent component analysis," in *IEEE Transactions on Neural Networks*, vol. 13, no. 6, pp. 1450-1464, Nov. 2002.

[12] M. M. Mukhedkar and S. B. Powalkar, "Fast face recognition based on Wavelet Transform on PCA," in *IEEE International Conference on Energy Systems and Applications*, Oct. 2015, pp. 761–764.

[13] M. Luo, L. Song and S. -d. Li, "An Improved Face Recognition Based on ICA and WT," *2012 IEEE Asia-Pacific Services Computing Conference*, Guilin, China, 2012, pp. 315-318.

[14] X. Zhihua and L. Guodong, "Weighted infrared face recognition in multiwavelet domain," *2013 IEEE International Conference on Imaging Systems and Techniques (IST)*, Beijing, China, 2013, pp. 70-74.

[15] A. Aldhahab, G. Atia, and W. B. Mikhael, "Supervised facial recognition based on multiresolution analysis with radon transform," in *2014 48th Asilomar Conference on Signals, Systems and Computers*, Nov. 2014, pp. 928–932.

[16] Y. Linde, A. Buzo, and R. Gray, "An Algorithm for Vector Quantizer Design," *IEEE Trans. Commun.*, vol. 28, no. 1, pp. 84–95, Jan. 1980.

[17] F. Z. Chelali, A. Djeradi, and N. Cherabit, "Investigation of DCT/PCA combined with Kohonen classifier for human identification," in *IEEE 4th International Conference on Electrical Engineering (ICEE)*, Dec. 2015, pp. 1–7.

[18] D. Li, H. Zhou, and K. M. Lam, "High-Resolution Face Verification Using Pore-Scale Facial Features,"

IEEE Trans. Image Process., vol. 24, no. 8, pp. 2317–2327, Aug. 2015.

[19] A. Aldhahab, T. A. Obaidi, and W. B. Mikhael, "Employing vector quantization on detected facial parts for face recognition," in *2016 IEEE Global Conference on Signal and Information Processing (GlobalSIP)*, Dec. 2016, pp. 1233–1237.

[20] A. Aldhahab, T. Alobaidi, A. Q. Althahab, and W. B. Mikhael, "Applying Multiresolution Analysis to Vector Quantization Features for Face Recognition," in *2019 IEEE 62nd International Midwest Symposium on Circuits and Systems (MWSCAS)*, Aug. 2019, pp. 598–601.

[21] S. J. Natu, P. J. Natu, T. K. Sarode, and H. B. Kekre, "Performance Comparison of Face Recognition Using DCT Against Face Recognition Using Vector Quantization Algorithms LBG, KPE, KMCG, KFCG," *Int. J. Image Process.*, vol. 4, no. 4, pp. 377–389, 2010.

[22] X. Duan and Z. H. Tan, "Local feature learning for face recognition under varying poses," in *IEEE International Conference on Image Processing (ICIP)*, Sep. 2015, pp. 2905–2909.

[23] J. Lu, V. E. Liong, and J. Zhou, "Simultaneous Local Binary Feature Learning and Encoding for Face Recognition," in *2015 IEEE International Conference on Computer Vision (ICCV)*, Dec. 2015, pp. 3721–3729.

[24] http://vision.ucsd.edu/content/yale-face-database

[25] https://www.nist.gov/programs-projects/face-recognition-technology-feret

[26] https://fei.edu.br/~cet/facedatabase.html

[27] http://www.anefian.com/research/face_reco.htm

[28] C. K. Chui, An introduction to wavelets, vol. 1. Academic press, 2014.

[29] V. Strela, P. N. Heller, G. Strang, P. Topiwala and C. Heil, "The application of multiwavelet filterbanks to image processing," in *IEEE Transactions on Image Processing*, vol. 8, no. 4, pp. 548-563, Apr. 1999,.

[30] V. Strela and A. T. Walden, "Orthogonal and biorthogonal multiwavelets for signal denoising and image compression," in *Wavelet Application V*, vol. 3391, pp. 96–107, SPIE, 1998.

[31] J. S. Geronimo, D. P. Hardin, and P. R. Massopust, "Fractal functions and wavelet expansions based on several scaling functions," *Journal of approximation theory*, vol. 78, no. 3, pp. 373-401, 1994.

[32] P. Rieder and J. A. Nossek, "Implementation of orthogonal wavelet transforms and their applications," in *Proceedings IEEE International Conference on Application-Specific Systems, Architectures and Processors*, 1997, pp. 489–498.

[33] K.-W. Cheung and L.-M. Po, "Preprocessing for discrete multiwavelet transform of two-dimensional signals," in *Proceedings IEEE International Conference on Image Processing*, 1997, vol. 2, pp. 350–353.

[34] D. P. Hardin and D. W. Roach, "Multiwavelet prefilters. 1. orthogonal prefilters preserving approximation order p\⩽ 2," *IEEE Trans. Circuits Syst. II Analog Digit. Signal Process.*, vol. 45, no. 8, pp. 1106–1112, 1998.

[35] A. Aldhahab, G. Atia, and W. B. Mikhael, "Supervised facial recognition based on multi-resolution analysis and feature alignment," in *2014 IEEE 57th International Midwest Symposium on Circuits and Systems (MWSCAS)*, 2014, pp. 137–140.

[36] A. Gersho and R. M. Gray, Vector quantization and signal compression. Boston, 1992.

[37] A. MAAFIRI and K. CHOUGDALI, "Face recognition using wavelets based feature extraction and PCA-L1 norm," in *2019 International Conference on Vision Towards Emerging Trends in Communication and Networking (ViTECoN)*, 2019, pp. 1–4.

[38] E. H. Hssayni and M. Ettaouil, "New Approach to Face Recognition Using Co-occurrence Matrix and Bayesian Neural Networks," in *2020 IEEE 6th International Conference on Optimization and Applications (ICOA)*, 2020, pp. 1–5.

[39] Y. Database, "Ucsd computer vision," 2022.

[40] P. J. Phillips, H. Wechsler, J. Huang, and P. J. Rauss, "The FERET database and evaluation procedure for face-recognition algorithms," *Image and Vision Computing*, vol. 16, no. 5, pp. 295–306, 1998.

[41] P. J. Phillips, Hyeonjoon Moon, S. A. Rizvi and P. J. Rauss, "The FERET evaluation methodology for face-recognition algorithms," in *IEEE Transactions on Pattern Analysis and Machine Intelligence*, vol. 22, no. 10, pp. 1090-1104, Oct. 2000.

[42] C. E. Thomaz and G. A. Giraldi, "A new ranking method for principal components analysis and its application to face image analysis," *Image and Vision Computing*, vol. 28, no. 6, pp. 902–913, 2010.

[43] A. S. B. Mahajan and K. J. Karande, "PCA and DWT based multimodal biometric recognition system," in *IEEE International Conference on Pervasive Computing (ICPC)*, Jan. 2015, pp. 1–4.

[44] A. Aldhahab, T. A. Obaidi, and W. B. Mikhael, "Employing vector quantization algorithm in a transform domain for facial recognition," in *2016 IEEE 59th International Midwest Symposium on Circuits and Systems (MWSCAS)*, Oct. 2016, pp. 1–4.

[45] A. Aldhahab, T. Alobaidi, and W. B. Mikhael, "Efficient facial recognition using vector quantization of 2D DWT features," in *2016 50th Asilomar Conference on Signals, Systems and Computers*, Nov. 2016, pp. 439–443.

Mustafa Rashid Ismael received the B.S. degrees in electrical engineering from the University of Babylon, Babel, Iraq, in 2004, the M.S. degree in electronic engineering from the University of Technology, Baghdad, Iraq, in 2011, and the Ph.D. degree in electrical and computer engineering from Western Michigan University, Kalamazoo, MI, USA, in 2018. He is currently working as an assistant professor at the Department of Electrical Engineering, University of Babylon, Babel, Iraq. His research interest includes image processing, pattern recognition, feature extraction, cognitive radio, and other signal processing problems.

Haider J. Abd earned his Ph.D. in the field of Electrical Engineering from University of Tenaga Nasional, Malaysia, 2014. He has more than fifteen years of experience in teaching. He completed his MSc, in Electrical Engineering, University of Baghdad, Baghdad, Iraq, 2005. He is currently working as a professor at the Department of Electrical Engineering, University of Babylon, Babel, Iraq. His research interests include optical fiber communication, Wireless communication, Computer Network, Digital signal processing, smart systems, Biomedical Engineering, Maglev system, and the Adaptive control system.